C–H Insertion Reactions of Nucleophilic Carbenes

by **Anthony J. Arduengo, III***[a]), **J. C. Calabrese**[b]), **Fredric Davidson**[b]), **H. V. Rasika Dias**[b])[1]), **Jens R. Goerlich**[b])[2]), **Roland Krafczyk**[a]), **William J. Marshall**[b]), **Matthias Tamm**[b])[3]), and **Reinhard Schmutzler**[a])

[a]) Institut für Anorganische und Analytische Chemie der Technischen Universität Carolo-Wilhelmina, Postfach 3329, D-38023 Braunschweig, Germany

[b]) *DuPont Science and Engineering Laboratory*, Experimental Station Wilmington, Delaware 19880, USA

Syntheses and characterizations are described for C–H insertion products derived from 1,3-dimesityldihydroimidazol-2-ylidene (**1**) with acetylene, acetonitrile, methyl phenyl sulfone, and chloroform. In the reaction with acetylene, both acetylenic H-atoms are reactive so that 1:1 and 2:1 adducts can be obtained. The acetylene and methyl-phenyl-sulfone adducts are structurally characterized by means of single-crystal X-ray structure determinations. The reactions of 1,3,4,5-tetramethylimidazolidin-2-ylidene (**8**) with chloroform or chlorodifluoromethane are shown to yield 2-(dihaloalkyl)imidazolium salts that arise from a failure of the intermediate 2-protioimidazolium salt to capture the initially formed halocarbanion.

Introduction. – The isolation, in recent years, of stable isolable carbenes has renewed interest in their chemical behavior [1–3]. Among the reactions commonly associated with carbenes is their X–H insertion reaction (X = C, N, O, S *etc.*). *Moss et al.* considered details of the O–H insertion reaction of dialkoxycarbene with various alcohols [4–6], and a recent treatment of this reaction by *Pezacki* has appeared [7]. These insertion reactions should be possible for both singlet electrophilic and singlet nucleophilic carbenes. The stepwise reaction pathway is expected to be different for carbenes of these two reactivity extremes (nucleophilic *vs.* electrophilic). There is also a middle ground of reactivity for biphilic carbenes where the insertion reaction can become concerted. These pathways as postulated by *Moss et al.* are presented in *Scheme 1* for a C–H insertion reaction.

Insertion reactions of imidazol-2-ylidenes, imidazolin-2-ylidenes (4,5-dihydroimidazol-2-ylidenes) or other strongly nucleophilic carbenes have not been widely studied, but a few examples can be found in the literature. *Wanzlick et al.* reported reactions of 1,3-diphenyldihydroimidazol-2-ylidene with acetophenone, benzaldehyde, cyclopentanone, furfural, nitromethane, or various sulfones [8–10]. These reactions appeared to have given C–H insertions, but identities of the products were not fully substantiated at the time, and mechanisms of their formation are unknown. It is also not clear whether these reactions originated from the carbene or its dimer. Some related O–H and N–H insertions of 1,3,4-triphenyl-1,2,4-triazol-5-ylidene have also been reported [11].

Because imidazolinylidene- and imidazolylidene-type carbenes are strongly nucleophilic singlet carbenes, they can be expected to react with compounds containing acidic C–H bonds according to the mechanism on the right in *Scheme 1*.

---

[1]) *DuPont* Visiting Scientist 1990–1992.

[2]) *DuPont* Visiting Scientist 1996–1997.

[3]) *DuPont* Visiting Scientist 1993–1994.

Scheme 1

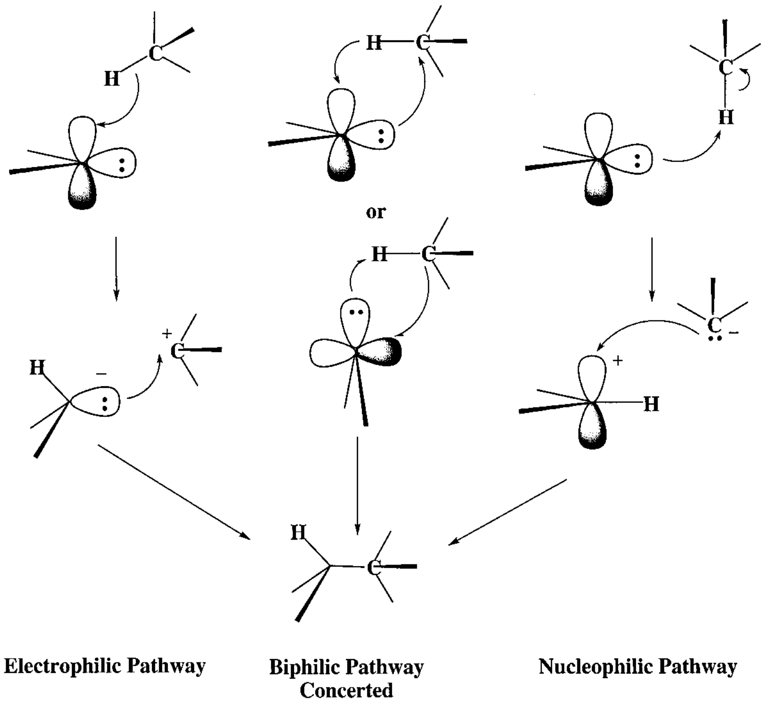

Results and Discussion. – The carbene 1,3-bis(2,4,6-trimethylphenyl)dihydroimidazol-2-ylidene (**1**) reacts with acetylene in a 1:1 ratio in THF at room temperature to form the C–H insertion product **2** (*Scheme 2*).

Scheme 2

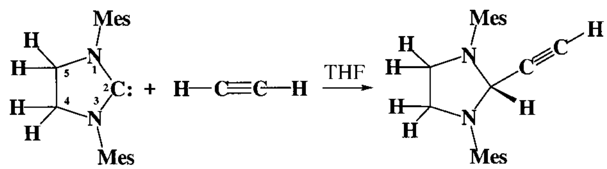

1 Mes = 2,4,6-trimethylphenyl **2**

Compound **2** is formed quantitatively and is isolated as colorless crystals, melting at 140–143° without decomposition. No other reaction involving the C≡C bond, such as a cycloaddition, is observed. The ^{13}C chemical shift for the former carbene center in **2** is at 69.0 ppm. This is an extremely high field shift with $\Delta\delta = 175.5$ ppm relative to the initial carbene **1**. The resonances for ^{13}C(4,5) of the imidazolidine ring of **2** (δ 50.5) is similar to the value observed in **1** (δ 51.3).

The H-atom at C(2) of **2** is observed as a *doublet* at 5.37 ppm with a small coupling (1.6 Hz) to the terminal acetylenic H-atom. This resonance is strongly upfield of the dihydroimidazolium *H*–C(2) atom of 1,3-bis(2,4,6-trimethylphenyl)imidazolium chloride which resonates at 9.0 ppm. The *doublet* for the acetylene H-atom appears at 2.33 ppm (^4J(H,H) = 1.6 Hz). The interior acetylene C-atom resonates at 84.9 ppm, and the terminal acetylenic C-atom (72.4 ppm) has a similar shift to that which we observe for acetylene (73.3 ppm) under the same conditions. Although the C_2 axial symmetry of the imidazolidine ring in **2** is broken by the addition of the acetylene residue at C(2), the pairs of *ortho*-Me groups, the *ortho*- and *meta*-C-atoms of the mesitylene rings appear as magnetically equivalent resonances at room temperature: 19.7 (*o*-Me), 130.2 (C_{meta}), 139.7 (C_{ortho}). A similar observation is also made from the ^{1}H-NMR spectrum, in which the *ortho*-Me groups exhibit a single resonance at 2.41 ppm, and the H-atoms at the *meta*-positions appear as a *singlet* at 6.84 ppm. However, due asymmetric substitution at C(2), an $AA'BB'$ system is observed for H–C(4,5) in **2** with signals at 3.42 and 3.73 ppm at room temperature. These observations suggest that, at room temperature, the mesityl (Mes) groups are able to freely rotate about the N–C bonds.

Indeed, low-temperature (– 80°) ^{1}H- and ^{13}C-NMR experiments on **2** reveal magnetically inequivalent resonances for most of the formerly identical *ortho*- and *meta*-pairs. In the ^{1}H-NMR spectrum, the *ortho*-Me groups resonate at 2.36 and 2.48 ppm (^{13}C-NMR 19.4 and 20.8 ppm). The pairs of Mes ring C-atoms also become inequivalent (130.23, 130.24 (C_{meta}); 137.9, 139.6 (C_{ortho})). However, the H-atoms at the *meta*-positions remain equivalent.

Crystals of **2** suitable for X-ray-diffraction studies were grown by cooling a saturated THF solution. The X-ray crystal structure of **2** is depicted by the KANVAS[4]) drawing in *Fig. 1*. Selected bond lengths and angles are given in the *Table*, along with structural parameters of related compounds.

The structure of **2** shows the expected tetrahedral geometry at the former carbene center (C(2)) with the acetylene moiety rising 130.4° out of the best plane of the imidazolidine ring. The C(2)–C bond distance is 147.0 pm. One nitrogen (N(1)) is

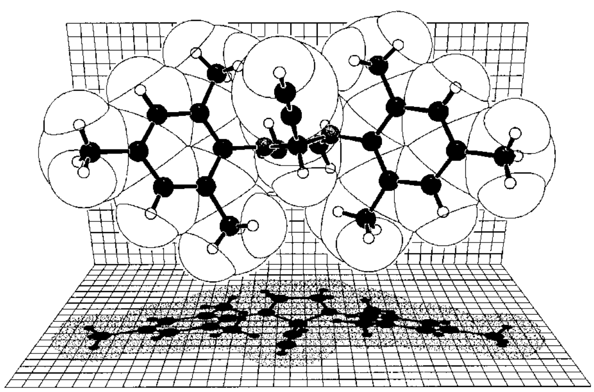

Fig. 1. *KANVAS Drawing of carbene-acetylene adduct* **2**

[4]) This drawing was made with the KANVAS computer graphics program. This program is based on the program SCHAKAL of *E. Keller* (Kristallographisches Institut der Universität Freiburg, Germany), which was modified by A. J. Arduengo, III, to produce the back and shadowed planes. The planes bear a 50-pm grid, and the lighting source is at infinity so that shadow size is meaningful.

Table 1. *Selected Bond Lengths* [pm] *and Angles* [°] *in* **2**–**4** *and the Carbene* **1**

Property	**1**	**2**[a])	**3**[b])	**4**
r(C(2)–N(3))	135.2(5), 134.5(5)	146.7(3), 145.3(3)	148.0(5), 148.0(5)	146.1(4), 164.5(5)
r(C(4)–C(5))	150.5(6)	145.8(4)	152.2(6)	148.2(5)
r(N(1,3)–C(4,5))	147.5(5), 148.7(5)	145.9(3), 139.7(3)	146.4(6), 147.2(5)	145.9(6), 139.8(6)
r(N(1,3)–C(Mes))	142.7(5), 143.7(5)	143.5(3), 142.6(3)	143.4(5), 144.6(5)	141.4(4), 141.6(4)
r(C(2)–C(1))	–	147.0(4)	148.1(6)	151.9(5)
Θ(N(1,3)–C(2)–C(1))	–	112.8(2), 114.0(2)	110.9(4), 115.5(4)	114.7(3), 109.3(3)
Θ(N(1)–C(2)–N(3))	104.7(3)	102.0(2)	101.9(3)	100.6(3)
Θ(C(5,4)–N(1,3)–C(2))	115.0(3), 114.6(3)	108.9(2), 112.0(2)	110.5(3), 110.3(4)	111.0(3), 113.2(3)
Θ(N(1,3)–C(5,4)–C(4,5))	101.6(4), 101.9(4)	105.6(2), 107.3(2)	102.3(3), 101.2(4)	105.3(3), 103.3(4)
Θ(C(2)–N(1,3)–C(Mes))	122.9(3), 122.5(3)	118.4(2), 121.5(2)	121.2(4), 121.6(3)	121.5(3), 121.9(3)

[a]) *r*(C≡C) = 117.6(3) pm. [b]) *r*(C≡C) = 121.2(9) pm.

strongly pyramidal and is displaced 30.9 pm above the plane of its three attached C-atoms (sum of the valence angles is 347.0°). The second N-atom, N(3), is much less pyramidal and lies only 3.7 pm below out of the plane of its attached C-atoms (sum of the valence angles is 359.8). The *anti*-orientation of the Mes substituents is apparent in the direct view of *Fig. 1*.

Aside from the pyramidalization of the N-atoms, the largest changes in the imidazole ring geometry upon insertion into the acetylene C–H bond occur at the C(2)-center. The bonds to the adjacent N-atoms both increase by *ca.* 10 pm in length relative to the initial carbene. These bond-length increases are greatest for the C-atoms attached to the most pyramidal N-atom which underscores the importance of σ-hybridization effects in these structures.

Compound **2** contains an additional acetylenic H-atom. This terminal C–H bond is also sufficiently acidic to undergo a carbene insertion reaction. The double insertion adduct **3** is formed from the reaction of **2** with an equivalent amount of carbene **1** in THF over a few days (*Scheme 3*).

Scheme 3

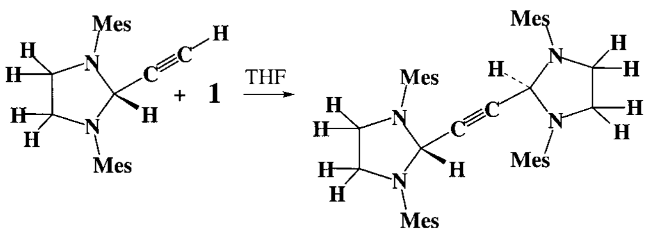

2 **3**

Compound **3** is also isolated in a high yield (86%) as colorless crystals, decomposing at 225°. No other by-products were detected by NMR.

The ^{13}C chemical shift for the former carbene centers in **3** (68.5; $\Delta\delta = 176$ ppm, relative to the carbene) have a high-field chemical shift like that observed in **2**. The C(4,5) and acetylene C-atom resonances are also similar to those observed in **2**. Remarkably, the *ortho*-Me groups and the *ortho*- and *meta*-C-atoms of the Mes rings of

3 each appear as magnetically equivalent resonances at room temperature in ^{13}C-NMR spectrum. As was the case for **2**, this equivalence is taken as an indication that the Mes groups in **3** can also freely rotate about their exocyclic C–N bonds at room temperature.

The ^{1}H-NMR spectrum of **3** also shows symmetry and chemical shifts similar to those observed in **2**. The *ortho*-Me groups show a single resonance at 2.03 ppm and the H-atoms at the *meta*-positions are equivalent with a resonance at 6.69 ppm. The H-atoms at C(4) and C(5) again show an *AA'BB'* pattern with *multiplets* centered at 3.20 and 3.50 ppm. The H-atom at C(2) in **3** appears as a *singlet* at 5.28 ppm.

Crystals of **3** suitable for X-ray diffraction studies were grown by cooling a THF solution to $-25°$. The solid-state structure of **3** is depicted by KANVAS drawing in *Fig. 2*. The molecule sits on a crystallographic mirror plane in the $P2_1/n$ space group. As in **2**, the structure of **3** shows the expected tetrahedral geometry at the former carbene centers (C(2)) with the acetylenic moiety inclined 128.7° out of the average plane of the imidazolidine ring and a C(2)–C bond distance of 148.1 pm. In contrast to **2**, both N(1) and N(3) are markedly pyramidal in **3**. The N(1) center lies 24.3 pm below the plane of its three attached C-substituents (sum of the valence angles is 351.2°), and N(3) rises

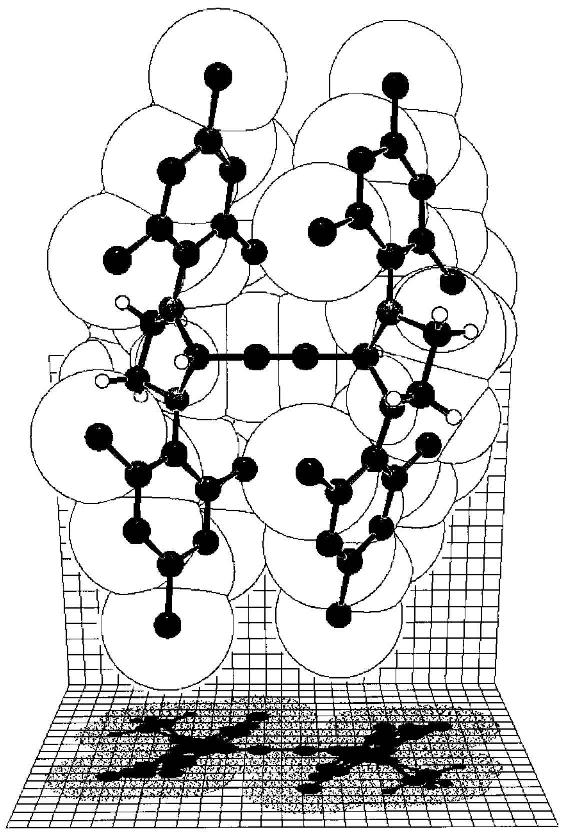

Fig. 2. *KANVAS Drawing of* **3**. Mesityl H-atoms are omitted for clarity.

19.0 pm above the plane of its attached C-atoms (sum of the valence angles is 354.6). The *anti*-orientation of the Mes substituents about the imidazolidine ring can be seen from the direct view of the drawing in *Fig. 2*.

As mentioned in the *Introduction*, *Wanzlick* and *Ahrens* examined the behavior of 1,3-diphenylimidazolin-2-ylidene with various sulfones [8]. The products of these reactions were postulated to arise from C–H insertion, but the products were characterized solely by their elemental analyses and melting points (for solids). Additionally, *Wanzlick*'s reactions were initiated from the dimer rather than the carbene. Thus, it was not clear if the products were formed directly from the dimer or if a carbene–carbene dimer preequilibrium was involved. The carbene **1** exists solely as the monomer with no tendency to dimerize under normal conditions. The reaction of 1,3-dimesityl-4,5-dihydroimidazol-2-ylidene (**1**) with methyl phenyl sulfone ($MeSO_2Ph$) is, therefore, a simplier system to study, and more complete characterization of the reaction product(s) is now possible.

The insertion of carbene **1** into an α-C–H bond of $MeSO_2Ph$ proceeds smoothly at room temperature in toluene to afford **4** as a colorless solid, melting at 189–94° (isolated 65%) (*Scheme 4*).

Scheme 4

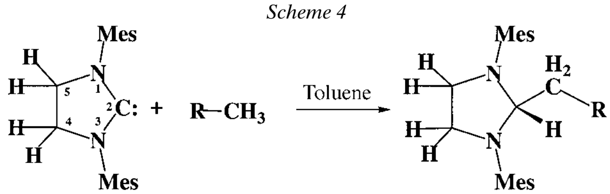

1

4 **R = PhSO₂**
5 **R = CN**

The ^{13}C chemical shift for the former carbene center is shifted to higher field (72.2 ppm) as is observed for the acetylene adducts **2** and **3**. The resonance for C(4,5) is at 50.3 ppm, and the methylene attached to C(2) resonates at 62.0 ppm. The *ortho*-Me groups of **5** appear as a broad resonance in the ^{13}C-NMR spectrum at room temperature at 19.6 ppm. In the ^{1}H-NMR spectrum, the H-atom at C(2) is observed as *triplet* at 5.55 ppm with a ^3J of 6.6 Hz to the $PhSO_2CH_2$ H-atoms. The CH_2(2) resonate as a *doublet* at 3.43 ppm (^3J(H,H) = 6.6 Hz). The H-atoms of *ortho*-Me groups are observed as magnetically inequivalent signals at 2.20 and 2.24 ppm, and the H-atoms at the *meta*-positions of the Mes groups are observed as a broad signal at 6.72 ppm. An *AA′BB′* system with *multiplets* centered at 3.09 and 3.29 ppm is observed for H–C(4) and H–C(5) (similar to **2** and **3**). These observations suggest that the $PhSO_2CH_2$ residue is too large to allow free rotation of the Mes groups at room temperature as had been observed for **2** and **3**.

Crystals of **4** suitable for X-ray-diffraction studies were grown from a THF/toluene mixture. The X-ray crystal structure of **4** is depicted by the KANVAS drawing in *Fig. 3*. The structure of **4** again shows the expected tetrahedral geometry at the former carbene center C(2) and a C(2)–C bond distance of 151.9 pm. The N(1) center lies 26.0 pm above the plane of the three attached C-atoms and is more pyramidal than

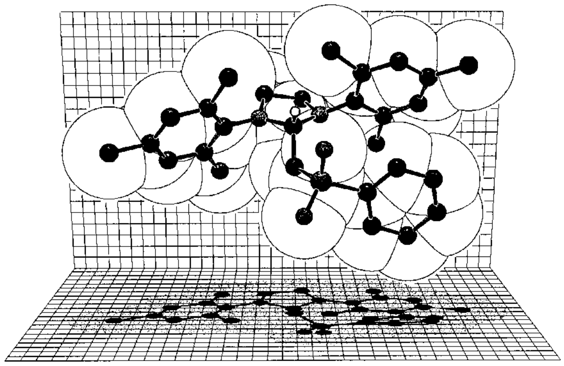

Fig. 3. *KANVAS Drawing of $MeSO_2Ph$ adduct* **4**

N(3), which is 12.6 pm below the plane of its C neighbors. The *anti*-orientation of the Mes substituents is also apparent from the direct view of the KANVAS drawing. There is an intramolecular stacking of the $PhSO_2$ residue with one of the Mes groups such that a set of ortho-C-atoms in the two rings approach one another at *ca.* 338.5 pm (C(12)–C(32)). This π-interaction does not appear to persist in solution as evidenced by the NMR data (*vide supra*).

Wanzlick and *Ahrens* also reported that C–H insertion reactions occur between dihydroimidazolylidenes (or their dimers) and MeCN or $PhCH_2CN$ [12]. Dissolving **1** in a solvent mixture of MeCN and toluene resulted in the insertion of the carbene in an MeCN C–H bond to form **5** (70%, M.p. 103°) as a colorless solid (*Scheme 4*).

The ^{13}C chemical shift for the former carbene center in **5** is 74.3 ppm ($\Delta\delta =$ 170.2 ppm higher field than observed in **1**). The imidazolidine C(4) and C(5) centers resonate at 51.0 ppm, and the C-atom attached to C(2) appears at 19.8 ppm. The nitrile C-atom (130.4 ppm) in **5** is 12.7 ppm downfield of the corresponding resonance in free Me*C*N (117.7 ppm). The *ortho*-Me groups, and the *ortho*- and *meta*-C-atoms of the Mes rings of **5** again appear as sets of magnetically equivalent resonances at room temperature (20.8 (*o*-Me), 135.7 (C_{meta}), 139.0 (C_{ortho})). The ^{1}H-NMR spectrum of **5** at room temperature also shows equivalent sets of resonances for the pairs of *ortho*- and *meta*-positions of the Mes groups as had been the case for the acetylene adducts **2** and **3**. As in compounds **2**–**4**, *H*–C(4) and *H*–C(5) appear as an *AA′BB′* system. The unique H-atom at C(2) is observed as *triplet* at 4.83 ppm with a coupling of 3.3 Hz to the CH_2CN H-atoms, which appear as a *doublet* at 1.65 ppm (^{3}J(H,H) = 3.3 Hz). Based on the room-temperature NMR spectra, the pendent Mes groups in **5** appear to freely rotate about the C–N bonds at room temperature.

In contrast to the reaction between **1** and MeCN, an unsaturated analog of **1**, 1,3-di(1-adamantyl)imidazol-2-ylidene (**6**), did not react with MeCN (*Scheme 5*).

Interestingly, when imidazol-2-ylidene **6** is recrystallized from MeCN or toluene/MeCN, the MeCN solvate of **6** is isolated, but there is no direct acetonitrile-imidazolylidene reaction or interaction. Solutions of **6** in CD_3CN do show H/D exchange for the *H*–C(4) and *H*–C(5), indicating that some equilibrium deprotonation reactions are occurring, but the carbene structure is otherwise unaltered. Similar exchanges are observed in (D_6)DMSO solutions. The acetonitrile anion is a stronger

Scheme 5

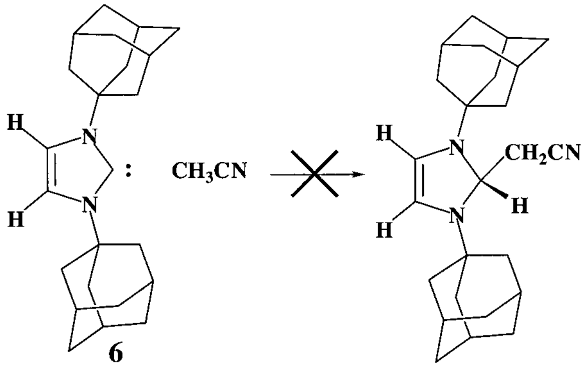

6

base than the carbene **6**. The structure of the imidazol-2-ylidene moiety in the 1:1 MeCN solvate of **6** is clearly indicative of the carbene [13], and the MeCN is also unperturbed. There is no evidence of C–H–C H-bonding between the carbene center and MeCN. The solid state orientation of the carbene **6** and its MeCN solvate is illustrated in *Fig. 4*.

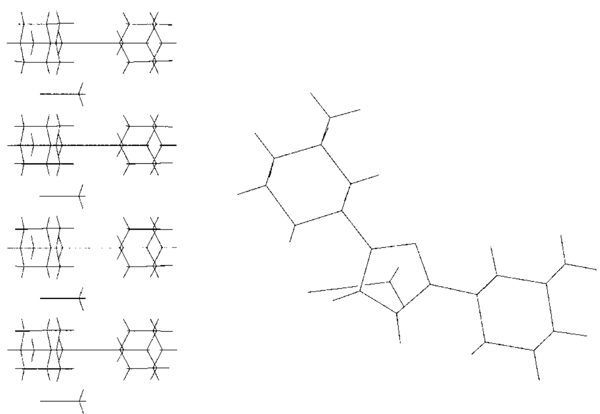

Fig. 4. *Packing of carbene* **6** *and MeCN along the* b *axis. Left-view:* perpendicular to *b*; *right-view:* down *b*.

The acetonitrile anion (generated by the deprotonation equilibria between **6** and MeCN) is not sufficiently nucleophilic to add to the highly stabilized 1,3-diadamantylimidazolium ion in order to form a C–H insertion product. However, when solutions of **6** in MeCN are heated for prolonged periods, a complex mixture of products is formed that appear to arise from the base catalyzed self-condensation of MeCN.

Wanzlick and co-workers employed an α-elimination reaction of $CHCl_3$ from 1,3-diphenyl-2-(trichloromethyl)imidazolidine as an entry point for their work directed toward stable carbenes [10][14][15]. Although *Wanzlick*'s work did not succeed in producing a stable imidazolinylidene, the corresponding dimers of the carbenes could be isolated. If transient carbenes were involved in *Wanzlick*'s α-elimination reaction, the reverse of this reaction (the C–H insertion of an imidazolinylidene with $CHCl_3$) may be possible starting with an isolated carbene (*Scheme 6*).

Scheme 6

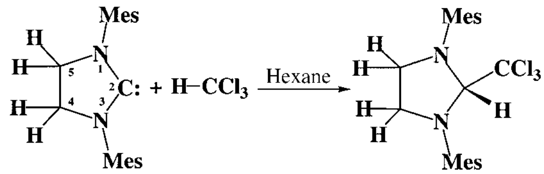

1 **7**

After 3 days at room temperature, carbene **1** added to $CHCl_3$ from a hexane solution to form the imidazolidine **7** (91%). Compound **7** is a colorless solid that melts at 172° with decomposition, most probably to carbene **1** and $CHCl_3$. The former carbene center C(2) in **7** has a lower field shift (86.5 ppm) than the C–H insertion adducts **2**–**5**. However, the centers C(4) and C(5) in **7** show a ^{13}C resonance (51.8 ppm) that is similar to the values for **2**–**5**. The C-atom of the Cl_3C group resonates at 108.6 ppm. The pairs of nuclei in *ortho*- and *meta*-positions of the Mes groups of **7** are magnetically inequivalent at room temperature and exhibit the largest shift differences of all the adducts in both ^1H- and ^{13}C-NMR spectra. Even the H-atoms at the *meta*-positions show resolved resonances with signals at 6.76 and 6.84 ppm. The H-atoms at C(4) and C(5) appear as an *AA'BB'* system with *multiplets* centered at 2.91 and 3.59 ppm. The H-atom at C(2) is observed as *singlet* at 5.66 ppm. These spectral observations suggest that the large Cl_3C moiety in **7** provides a substantial barrier to rotation of the Mes rings and creates a distinctive magnetic environment for groups positioned above and below the average imidazolidine plane.

The C–H insertion of $CHCl_3$ with dihydroimidazolylidenes was never reported by *Wanzlick* but offers a complement to his earlier work. It is tempting and even reasonable to view the additions of compounds like acetylene ($pK_a \approx 25$), $MeSO_2Ph$ ($pK_a \approx 22$), and MeCN ($pK_a \approx 25$) to a strongly nucleophilic carbene like **1** as occurring by an ionic mechanism (the pathway to the right in *Scheme 1*). The acidity of $CHCl_3$ ($pK_a \approx 25$) also makes it a reasonable candidate for such a reaction pathway. There is, however, a complication in the case of $CHCl_3$ that does not arise with the other C–H acids mentioned above. That complication is the potential α-elimination of Cl^- from a transient Cl_3C^- anion that would be involved in the putative stepwise C–H insertion process. Previous reports of the reaction of carbene **1** with CCl_4 demonstrated that, by an apparent ionic pathway (radicals or electron transfer in this reaction were not detected), Cl^+ could be transferred from CCl_4 to the carbene **1** with the liberation of a Cl_3C^- anion (*Scheme 7*) [16]. However, the potential product 2-chloro-1,3-dimesityl-2-(trichloromethyl)imidazolidine (the C–Cl insertion product) was not observed, but rather the CCl_3^- anion rather undergoes an α-elimination of chloride to produce dichlorocarbene that, in turn, reacts with additional carbene **1**.

The yield (91%) of the insertion product **7** from $CHCl_3$ and carbene **1** is among the highest that we have observed of such insertion reactions. Obviously, α-elimination pathways from the Cl_3C^- anion are not very important for this reaction. Additionally, we note that *Wanzlick* never reported the detection of any products that could be

Scheme 7

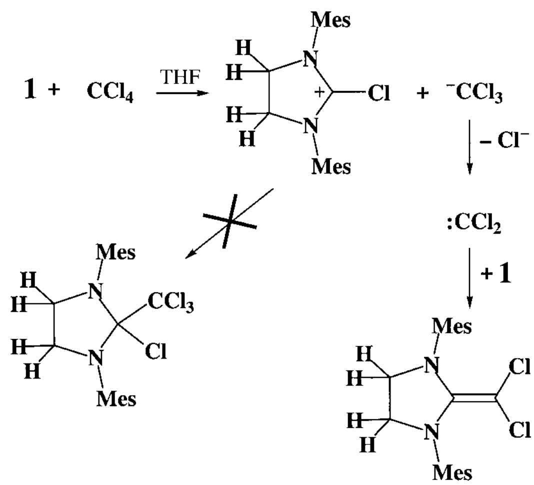

attributed to the intermediacy of dichlorocarbene from his 2-(trichloromethyl)imidazolidine α-eliminations. These observations suggest that the C–H insertion of **1** into $CHCl_3$ and the reverse reaction (α-elimination of $CHCl_3$ from 2-(trichloromethyl)-imidazolidines) may not involve free Cl_3C^- anion, and that there may be some measure of concertedness in these reactions. This would suggest a mechanism that is intermediate between the center and right pathways in *Scheme 1*. The observation that the CCl_4 reaction (*Scheme 7*) does involve the Cl_3C^- anion (and its subsequent α-elimination to form dichlorocarbene) is consistent with the requirement that nucleophilic displacement at Cl has a strong preference for a linear transition-state geometry at Cl (*Scheme 8*) [17][18]. Deprotonations, on the other hand, show a much more flexible transition-state geometry, so that a pathway with some degree of concert becomes possible (*Scheme 8*) [19][20].

Scheme 8

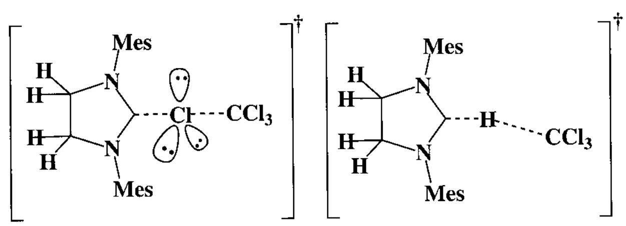

The character of a nucleophilic carbene – $CHCl_3$ insertion reaction can be changed if the ability of the (dihydro)imidazole fragment to accept a nucleophile at C(2) is altered. Indeed when 1,3,4,5-tetramethylimidazol-2-ylidene reacts with $CHCl_3$ or $CHClF_2$, a different reaction pathway is followed that produces a 2-(dihalomethyl)imidazolium salt as the major product (*Scheme 9*).

The reaction of 1,3,4,5-tetramethylimidazol-2-ylidene (**8**) with $CHCl_3$ in THF leads to a 80:20 mixture of the dichloromethylimidazolium chloride **10 · Cl** and 1,3,4,5-

Scheme 9

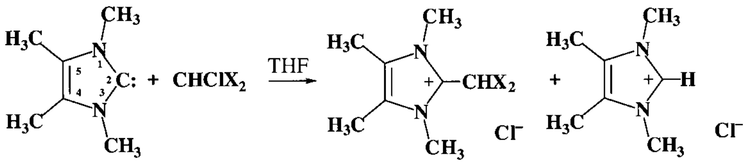

8

10·Cl X = Cl
11·Cl X = F

9·Cl

tetramethylimidazolium chloride (**9·Cl**). The low yield of 2-hydroimidazolium chloride is presumed to arise from dichlorocarbene that is lost to side reactions (dimerization and reaction with solvent). An analogous reaction occurs between 1,3,4,5-tetramethylimidazol-2-ylidene and $CHClF_2$, except the yield of **9·Cl** is reduced to *ca.* 15%. These reactions are believed to proceed according to *Scheme 10*.

Scheme 10

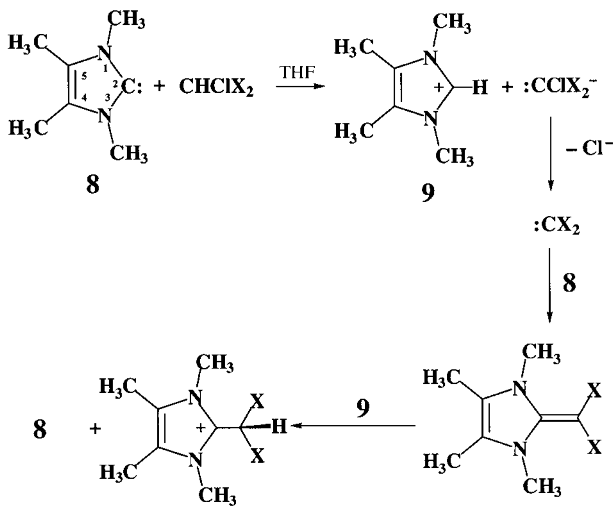

10 X = Cl
11 X = F

12 X = Cl
13 X = F

Simplistically, the cations **10** and **11** appear to arise from S_N2 displacement reactions of the nucleophilic carbene **8** on $CHCl_3$ or $CHClF_2$. It is, however, well recognized that the barrier for these direct displacements is high and such substitution reactions actually occur through dihalocarbene intermediates [21–24]. Therefore, **10** and **11** most probably arise *via* the mechanism proposed in *Scheme 10*.

A key step in the formation of the 2-(dihalomethyl)imidazolium ions **10** and **11** is the deprotonation of the 2-hydroimidazolium ion **9** by the olefin (**12** or **13**) to regenerate the carbene **8** and produce the final substituted imidazolium ion **10** (or **11**). For an imidazole ring system, this reaction proceeds as depicted in *Scheme 10*, because the 2-methylideneimidazole (**12** or **13**) is more basic than the corresponding carbene

(**8**). For 2-methylideneimidazolines and their corresponding carbenes (imidazolin-2-ylidenes, *e.g.*, **1**), the carbene is more basic than the olefin. These basicity relationships hold as long as the substituents X are not strong π-acceptors [25] (see [17] for leading information).

Because the 2-hydroimidazolium ion (**9**) in the process illustrated by *Scheme 10* is stabilized by extensive π-delocalization, a trihalomethyl anion is not readily added to C(2). Instead, the trihalomethyl anion persists in various proton-transfer equilibria until it suffers α-chloro elimination to produce a dihalocarbene. Thus, for simple imidazol-2-ylidenes a C–H insertion of hydrocarbon acids like $CHCl_3$, acetylene, or active methylene compounds does not occur.

The solid-state structure of the 2-(dichloromethyl)imidazolium ion **10** (as its tetraphenylborate salt, **10 · BPh₄**) is illustrated by the KANVAS drawing in *Fig. 5*. The $CHCl_2$ substitution on the imidazole ring as predicted by the mechanism in *Scheme 10* is evident. The $CHCl_2$ residue adopts an orientation that minimizes the steric interaction between Cl-atoms and the *N*-Me groups. In this orientation, the methine H-atom is not aligned to hyperconjugate with the imidazolium fragment. For the chloride salt **10 · Cl** in MeCN, the methine H-atom resonates at 8.64 ppm in the ^{1}H-NMR spectrum. The corresponding tetraphenylborate salt **10 · BPh$_4$** shows this methine resonance at 7.39 ppm.

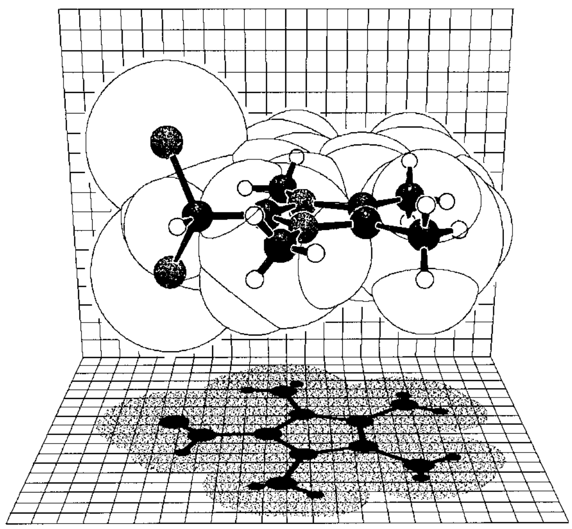

Fig. 5. *KANVAS Drawing of* **10** (in **10 · BPh$_4$**).

The structure of the salt **11 · Cl** is illustrated in *Fig. 6*. The CHF_2 group in **11 · Cl** adopts an orientation that is related to that observed for **10 · BPh$_4$** such that the methine H-atom again lies in the plane of the imidazole ring. Even though the methine proton does not benefit from enhanced acidity through hyperconjugation with the imidazolium ion, there is a H-bonding interaction between the Cl^- gegenion and the methine H-atom. The Cl–H–C angle is 150° with Cl–H and H–C distances of 256 and 97 pm, respectively.

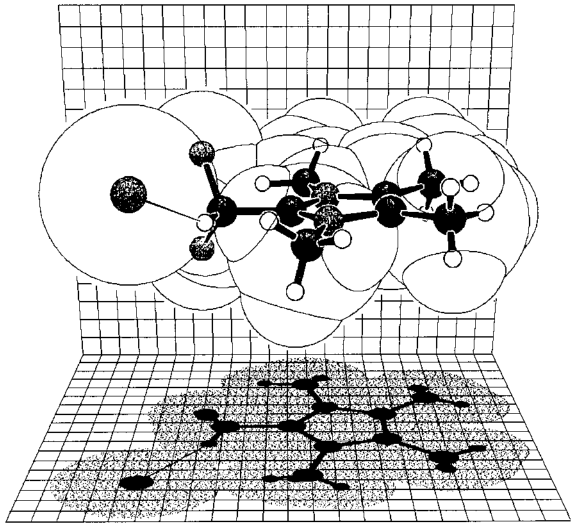

Fig. 6. *KANVAS Drawing of* **11** · **Cl**.

The chemical shift of the methine H-atom in **11** is also strongly counterion dependent. The chloride salt **11** · **Cl** exhibits the methine resonance at 7.99 ppm (MeCN), whereas, in the tetraphenylborate salt, the resonance occurs at 7.18 ppm (MeCN). These large counterion chemical-shift dependencies in **10** and **11** suggest that some of the anion-cation (H-bonding) interactions that are observed in the solid state may also persist to some extent in solution.

Conclusions. – C–H Insertion reactions of imidazolin-2-ylidenes do occur with acidic C–H bonds. These reactions are consistent with a stepwise pathway proposed by *Moss et al.* for strongly nucleophilic carbenes. There may be some degree of concertedness to these insertions, because evidence is not observed for the free anions that would be formed by a fully stepwise process. Further work is necessary to conclusively demonstrate whether a stepwise or concerted process best describes these insertions. Imidazol-2-ylidenes undergo stepwise C–H and C–C bond forming reactions with $CHCl_3$ or $CHClF_2$, but these reactions do not result in a net C–H insertion product, because the initially formed trihalocarbanion is not captured by the first-formed imidazolium ion.

A.J.A., *R.K.*, and *R.S.* thank the *DuPont Company* for their support of portions of this work (Contribution Nr. 7672). *R.K.* gratefully acknowledges the support of *DuPont* and the *Universität Braunschweig* that enabled a visit to the *DuPont Experimental Station*. *A.J.A.* is grateful to the *Alexander von Humboldt Stiftung* for a senior research prize that facilitated this work.

Experimental Part

General. Reactions and manipulations were carried out under an atmosphere of dry N_2, either in a *Vacuum Atmospheres* dry box or using standard *Schlenk* techniques. Solvents were dried (by standard procedures), distilled, and deoxygenated prior to use, unless otherwise indicated. Glassware was oven-dried at 160° overnight. ^{1}H-NMR: *General Electric QE-300* and *GE Omega 300WB* spectrometer. ^{13}C- and ^{15}N-NMR: *GE Omega*

300WB spectrometer. NMR References are Me_4Si (^{1}H, ^{13}C) and $NH_4^+NO_3^-$ (^{15}N). Mass spectra were obtained with a *VG-ZAB-E* mass spectrometer. M.p. were obtained on a *Thomas-Hoover* capillary apparatus or on a *Laboratory Devices Mel-Temp II* apparatus, and were not corrected. Elemental analyses were performed by *Micro-Analyses Inc.,* Wilmington, Delaware, or *Oneida Research Services*, Whitesboro, NY.

1,3-Bis(2,4,6-trimethylphenyl)-2-(ethynyl)imidazolidine (**2**). To a soln. of 1.0 g (3.26 mmol) of *1,3-bis(2,4,6-trimethylphenyl)-4,5-dihydroimidazol-2-ylidene* (**1**) in 10 ml of THF were condensed 93 mg (3.59 mmol) of acetylene at $-196°$.The colorless mixture was allowed to warm to 23° and was stirred for 16 h, during which time it became yellow. The solvent and all volatiles were removed *in vacuo*, and the resulting oil was recrystallized from THF at $-25°$to afford **2** as colorless crystals, which were suitable for X-ray diffraction. Yield: 1.016 g (93%). M.p. 140–3°. ^{1}H-NMR ((D_8)THF): 2.22 (*s*, *p*-Me); 2.33 (*d*, ^4J(H,H) = 1.62, C≡C*H*); 2.41 (*s*, 4 *o*-Me); 3.42 (*m*, NCH_2); 3.73 (*m*, NCH_2); 5.37 (*d*, ^4J(H,H) = 1.62, H–C(2)); 6.84 (*s*, 2*m*-CH). ^{13}C{^{1}H}-NMR ((D_8)THF): 19.74 (*s*, *o*-Me); 20.97 (*s*, *p*-Me); 50.54 (*s*, NCH_2); 68.96 (*s*, C(2)); 72.38 (*s*, C≡*C*H); 84.87 (*s*, *C*≡CH); 130.23 (*s*, C_m); 135.95 (*s*, C_p); 139.18 (br. *s*, C_{ipso}); 139.72 (*s*, C_o). ^{13}C-NMR ((D_8)THF): 19.74 (*qm*, ^1J(C,H) = 126.34, *o*-Me); 20.97 (*tq*, ^1J(C,H) = 125.73, ^3J(C,H) = 4.58, *p*-Me); 50.54 (*t*, ^1J(C,H) = 140.23, NCH_2); 68.96 (*dm*, ^1J(C,H) = 150.15, C(2)); 72.37 (*dd*, ^1J(C,H) = 148.42, ^3J(C,H) = 3.66, C≡*C*H); 84.87 (*dd*, ^2J(C,H) = 47.61, ^2J(C,H) = 2.45, *C*≡CH); 130.23 (*dm*, ^1J(C,H) = 153.82, C_m); 135.95 (*q*, ^2J(C,H) = 5.49, C_p); 139.18 (*m*, C_{ipso}); 139.72 (*m*, C_o). ^{15}N-NMR ((D_8)THF): -328.38 (*s*). ^{1}H-NMR ((D_8)THF, $-80°$): 2.364 (*s*, 2 *o*-Me); 2.438 (*s*, 2 *o*-Me); 2.23 (*s*, 2 *p*-Me); 2.75 (*d*, ^4J(H,H) = 1.20, C≡C*H*); 3.36 (*m*, NCH_2); 3.74 (*m*, NCH_2); 5.29 (br. *s*, H–C(2)); 6.86 (*s*, 4 *m*-CH). ^{13}C{^{1}H}-NMR ((D_8)THF, $-80°$): 19.383 (*s*, *o*-Me); 20.772 (*s*, *o*-Me); 21.071 (*s*, *p*-Me); 50.697 (*s*, NCH_2); 74.500 (*s*, C(2)); 72.642 (*s*, C≡*C*H); 85.517 (*s*, *C*≡CH); 130.231 (*s*, C_m); 130.237 (*s*, C_m); 135.779 (*s*, C_p); 139.463 (*s*, C_{ipso}); 137.912 (*s*, C_o); 139.624 (*s*, C_o). Anal. calc. for $C_{23}H_{28}N_2$ (332.49): C 83.09, H 8.49, N 8.43; found: C 83.21, H 8.50, N 8.21.

1,2-Bis[1,3-bis(2,4,6-trimethylphenyl)imidazolidin-2-yl]ethyne (**3**). A soln. of 100 mg (0.301 mmol) of **2** and 92 mg (0.301 mmol) of **1** in 10 ml of THF was stirred for 3 d at 23°. The solvent volume was reduced *in vacuo* and the clear yellow solution stored at $-25°$ to induce crystallization of **3** as colorless crystals. Yield: 165 mg (86%). M.p. 233–5° (225° dec.). ^{1}H-NMR ((D_8)THF): 2.03 (*s*, 8 *o*-Me); 2.29 (*s*, 4 *p*-Me); 3.20 (*m*, 2 NCH_2); 3.50 (*m*, 2 NCH_2); 5.28 (*s*, 2 H–C(2)); 6.69 (*s*, 8 *m*-CH). ^{13}C{^{1}H}-NMR ((D_8)THF): 19.34 (*s*, *o*-Me); 21.10 (*s*, *p*-Me); 50.62 (*s*, NCH_2); 68.53 (*s*, C(2)); 84.52 (*s*, C≡*C*); 130.35 (*s*, C_m); 135.21 (*s*, C_p); 139.03 (br. *s*, C_{ipso}); 139.67 (*s*, C_o). Anal. calc. for $C_{44}H_{54}N_4$ (638.94): C 82.71, H 8.52, N 8.77; found: C 82.83, H 8.54, N 8.66.

1,3-Bis(2,4,6-trimethylphenyl)-2-[(phenylsulfonyl)methyl]imidazolidine (**4**). A soln. of 102 mg (0.33 mmol) of **1** and 55 mg (0.33 mmol) of $MeSO_2Ph$ in 30 ml of toluene was stirred for 20 h at 23°. Evaporation of the volatiles gave a brown oil, which upon recrystallization from hexane furnished a colorless solid. Yield: 100 mg (65%). M.p. 189–94°. Solns. in CD_2Cl_2 decomposed. ^{1}H-NMR (C_6D_6): 2.12 (*s*, 2 *p*-Me); 2.20, 2.24 (*s*, 2 *o*-Me); 3.09 (*m*, NCH_2); 3.29 (*m*, NCH_2); 3.43 (*d*, ^3J(H,H) = 6.6, C$H_2$$SO_2$Ph); 5.55 (*t*, ^3J(H,H) = 6.6, H–C(2)); 6.5–7.7 (*m*, 5 H, Ph); 6.72 (*s*, 4 *m*-CH). ^{13}C-NMR (C_6D_6): 19.64 (br. *s*, *o*-Me); 20.88 (*s*, *p*-Me); 50.27 (*s*, NCH_2); 62.03 (*s*, CH_2SO_2Ph); 72.16 (*s*, C(2)); 127.62, 128.70, 132.31, 135.46, 136.66, 137.90, 139.07, 140.68 (8*s*, arom. C). EI-MS (70 eV): 463.2414 (5, $[M+H]^+$; calc.: 463.2419), 462.2340 (5), M^+; calc. for $C_{28}H_{34}N_2O_2S$: 462.2341), 324.2184 (15, $[M-C_7H_6OS]^+$; calc.: 324.2201], 305.1938 (40, $[M-C_7H_9O_2S]^+$; calc.: 305.2018), 148.1119 (100, $[C_{10}H_{14}N]^+$; calc.: 148.1126).

1,3-Bis(2,4,6-trimethylphenyl)-2-(cyanomethyl)imidazolidine (**5**). A soln. of 0.275 g (0.900 mmol) of **1** in a mixture of 5 ml of toluene and 5 ml of MeCN was stirred for 2 h at 23°. The mixture was concentrated *in vacuo* to give a yellow oily soln. that did not crystallize upon storage at $-25°$. A few drops of hexane were added, whereupon storage at $-25°$ led to the formation of a colorless solid, which was collected by filtration and dried *in vacuo*. Yield: 0.22 g (70%). M.p. 103°. ^{1}H-NMR (C_6D_6): 1.65 (*d*, ^3J(H,H) = 3.3, CH_2CN); 2.13 (*s*, 4 *o*-Me); 2.53 (br. *s*, 2 *p*-Me); 3.0 (*m*, NCH_2); 3.5 (*m*, NCH_2); 4.83 (*t*, ^3J(H,H) = 3.3, H–C(2)); 6.7–7.0 (*m*, 4 *m*-CH). ^{13}C-NMR (C_6D_6): 19.80 (br. *s*, CH_2CN); 20.79 (*s*, *o*-Me); 23.37 (*s*, *p*-Me); 51.03 (*s*, NCH_2); 74.34 (*s*, C(2)); 129.93 (*s*, C_p); 130.39 (br., CN); 135.68 (*s*, C_m); 139.04 (*s*, C_o); 142.91 (*s*, C_{ipso}). EI-MS (70 eV): 347.2360 (10, *M*; calc. for $C_{23}H_{29}N_3$: 347.2362), 307.2182 (100, $[M-CH_2CN]^+$; calc.: 307.2174), 148.1124 (50, $C_{10}H_{14}N^+$; calc.: 148.1126).

1,3-Bis(2,4,6-trimethylphenyl)-2-(trichloromethyl)imidazolidine (**7**). To a soln. of 0.153 g (0.500 mmol) of **1** in 20 ml of hexane was added a soln. of 3.60 g (3.00 mmol) of $CHCl_3$ in 5 ml of hexane. The mixture was stirred for 80 h at 23°. Evaporation of the volatiles yielded **7** as a colorless solid which was recrystallized from hexane/Et_2O at $-20°$. Yield: 0.194 g (91%). M.p. 172° (dec.). ^{1}H-NMR (C_6D_6): 2.14 (*s*, 2 *p*-Me); 2.34, 2.49 (2*s*, 4 *o*-Me); 2.8 (*m*, NCH_2); 3.7 (*m*, NCH_2); 5.66 (*s*, H–C(2)); 6.76, 6.84 (2*s*, 4 *m*-CH). ^{13}C-NMR (C_6D_6): 20.17, 20.76 (2*s*, *o*-Me); 21.43 (*s*, *p*-Me); 51.81 (*s*, NCH_2); 86.46 (*s*, C(2)); 108.57 (*s*, Cl_3C); 130.17, 130.46 (2*s*, C_m); 133.95, 134.83 (2*s*, C_o); 138.20 (*s*, C_p); 141.77 (*s*, C_{ipso}). EI-MS (70 eV): 353.1846 (5, $[M-2\ Cl-H]^+$; calc. for $C_{22}H_{26}ClN_2$:

353.1785), 307.2292 (95, $[M - CCl_3]^+$; calc.: 307.2174), 305.2154 (100, $[M - CHCl_3 - H]^+$; calc.: 305.2018). FAB-MS (NBA): 425.15 (5, M^+; calc. for $C_{22}H_{27}Cl_3N_2$; 425.15), 307.23 (100, $[M - CCl_3]^+$).

2-(Dichloromethyl)-1,3,4,5-tetramethylimidazolium Chloride (**10 · Cl**): $CHCl_3$ (1.0 g, 8.4 mmol) was condensed onto a cooled (liquid N_2) soln. of *1,3,4,5-tetramethylimidazol-2-ylidene* (**8**; 1.0 mg, 8.0 mmol) in 50 ml of THF. The mixture was allowed to warm to $-78°$ and stirred to insure complete mixing. The mixture became red and produced a precipitate. After 30 min the mixture was allowed to warm to 23° and stirred for an additional 15 min. The precipitate was isolated by filtration and washed with THF and Et_2O. A dark green powder was obtained. NMR showed a *ca.* 4 : 1 mixture of **10 · Cl** and *1,3,4,5-tetramethylimidazolium chloride* (**9 · Cl**). Pure **10 · Cl** was obtained by crystallization from an MeCN soln. at $-26°$. Yield: 910 mg (46%). M.p. 218–20°. ^{1}H-NMR (CD_3CN): 2.24 (*s*, 2 MeC); 3.96 (*s*, 2 MeN); 8.64 (*s*, $CHCl_2$). Anal. calc. for $C_8H_{13}Cl_3N_2$ (243.56) C 39.45, H 5.38, N 11.50; found: C 40.34, H 5.61, N 12.07.

2-(Dichloromethyl)-1,3,4,5-tetramethylimidazolium Tetraphenylborate (**10 · BPh_4**). A soln. of **10 · Cl** (1.5 g, 6.0 mmol) in 50 ml of H_2O was treated with a filtered soln. of $NaBPh_4$ (2.2 g, 6.0 mol) in 50 ml of H_2O. After stirring for 1 h, the greenish precipitate was isolated by filtration and washed with H_2O. The resulting greenish powder was dried at 80° under high vacuum for 16 h. Yield: 2.93 g (90%). M.p. > 250°. ^{1}H-NMR (CD_3CN): 2.23 (*s*, 2 MeC); 3.82 (*s*, 2 MeN); 6.84 (*tt*, 4 H–C(4) (Ph)); 6.99 (*t*, 4 H–C(3), 4 H–C(5)(Ph)); 7.27 (*m*, 4 H–C(2), 4 H–C(6)(Ph)); 7.39 (*s*, $CHCl_2$). ^{13}C-NMR (CD_3CN): 8.94 (*s*, *Me*); 34.14 (*s*, *Me*); 56.76 (*s*, $CHCl_2$); 122.75 (*q*, $J(^{13}C,^{11}B) = 0.6$, C(4)(Ph)); 126.58 (*q*, $J(^{13}C,^{11}B) = 2.8$, C(3), C(5)(Ph)); 130.40 (*s*, NC*C*N); 136.71 (*q*, $J(^{13}C,^{11}B) = 1.5$, C(2), C(6)(Ph)); 137.32 (*s*, NCN); 164.83 (*q + sept.*, $J(^{13}C,^{11}B) = 49.6$, $J(^{13}C,^{10}B) = 16.5$, C_{ipso}).

2-(Difluoromethyl)-1,3,4,5-tetramethylimidazolium Chloride (**11 · Cl**). $CHClF_2$ (112 ml, 5.00 mmol) was condensed onto a cooled (liq. N_2) soln. of **8** (621 mg, 5.00 mmol) in 50 ml of THF. The mixture was allowed to warm to 23°. A cream-colored precipitate formed almost immediately and was collected by filtration, and washed with THF and Et_2O. Yield: 910 mg (6 : 1 mixture of **11 · Cl** and **9 · Cl**). Pure **11 · Cl** was obtained by several fractional crystallizations from MeCN at $-26°$. M.p. 204–218°. ^{1}H-NMR (CD_3CN): 2.26 (*t*, $J(^{19}F,^1H) =$ 0.9, 2 MeC); 3.87 (*t*, $J(^{19}F,^1H) = 0.9$ MeN); 7.99 (*t*, $J(^{19}F,^1H) = 0.9$, 2 MeC); 3.87 (*t*, $J(^{19}F,^1H) = 0.9$ MeN); 7.99 (*t*, $J(^{19}F,^1H) = 49$, CHF_2). ^{13}C-NMR (CD_3CN): 8.83 (*s*, *Me*C); 34.09 (*s*, MeN); 107.06 (*t*, $^1J(^{19}F,^{13}C) = 238$, CHF_2); 130.70 (*s*, NC*C*N); 134.80 (*t*, $J(^{19}F,^{13}C) = 29.9$, NCN). ^{19}F-NMR (CD_3CN): 117.81 (*d*, $J(^{19}F,^1H) = 49$). Anal. calc. for $C_8H_{13}ClF_2N_2$ (210.07): C 45.61, H 6.22, N 13.30; found: C 45.87, H 5.84, N 13.01.

2-(Difluoromethyl)1,3,4,5-tetramethylimidazolium Tetraphenylborate (**11 · BPh_4**). A soln. of **11 · Cl** (335 mg, 1.6 mmol) in 30 ml of H_2O was treated with a filtered soln. of $NaBPh_4$ (600 mg, 1.75 mmol) in 20 ml of H_2O. Stirring was continued overnight, and the white precipitate was isolated by filtration and washed with H_2O. The resulting white powder was dried under vacuum at 80° for 16 h. Quant. yield. M.p. 269–3°, ^{1}H-NMR (CD_3CN): 2.24 (*s*, 2 MeC); 3.76 (*s*, 2 MeN); 6.84 (*tt*, 4 H–C(4)(Ph)); 6.99 (*t*, 4 H–C(3), 4 H–C(5)(Ph)); 7.18 (*t*, $J(^{19}F,^1H) = 49$, CHF_2); 7.27 (*m*, 4 H–C(2), 4 H–C(6)(Ph)). ^{13}C-NMR (CD_3CN): 8.76 (*s*, *Me*C); 33.73 (*t*, $J(^{19}F,^{13}C) = 2.1$, MeN); 106.45 (*t*, $^1J(^{19}F,^{13}C) = 238$, CHF_2); 122.74 (*m*, C(4)(Ph)); 126.58 (*m*, C(3), C(5)(Ph)); 130.79 (*s*, NC*C*N); 134.05 (*t*, $J(^{19}F,^{13}C) = 29.9$, N*C*N); 136.70 (*m*, C(2), C(6)(Ph)); 164.78 (*m*, C(1)(Ph)). Anal. calc. for $C_{32}H_{33}BF_2N_2$ (494.43): C 77.74, H 6.73, N 5.67; found: C 79.15, H 6.14, N 5.43.

Crystal Data for **2**. At $-100°$ with MoK_α radiation: $a = 727.0(1)$, $b = 1594.7(1)$, $c = 3357.5(1)$ pm, orthorhombic, *Pbca*, $Z = 8$, $\mu(Mo) = 0.62$ cm^{-1}, 2060 unique reflections with $I > 3\sigma(I)$. The structure was solved by direct methods (MULTAN) and refined by full-matrix least-squares analysis on *F*. C and N were refined with anisotropic thermal parameters. H-Atoms were modeled in fixed positions. The largest residual electron density in the final difference *Fourier* map was 0.22 e/Å^3 near H(17′). The data/parameter ratio was 9.10. The final *R* factors were $R = 0.052$ and $R_w = 0.054$. Crystallographic data for the structure of **2** have been deposited with the *Cambridge Crystallographic Data Centre* (*CCDC*) (No. 133399). Copies of the data can be obtained free of charge on application to the CCDC, 12 Union Road, Cambridge CB21EZ, UK (fax: +44(1223)336-033; e-mail: teched@chemcrys.cam.ac.uk).

Crystal Data for **3**. At $-100°$ with MoK_α radiation: $a = 839.6(3)$, $b = 2025.2(4)$, $c = 1170.7(3)$ pm, $\beta =$ 110.04(2)°, monoclinic, $P2_1/n$, $Z = 2$, $\mu(Mo) = 0.62$ cm^{-1}, 1212 unique reflections with $I > 3\sigma(I)$. The structure was solved by direct methods (MULTAN) and refined by full-matrix least-squares analysis on *F*. C and N were refined with anisotropic thermal parameters. H-Atoms were modeled in fixed positions. The largest residual electron density in the final difference *Fourier* map was 0.18 e/Å^3. The data/parameter ratio was 5.57. The final *R* factors were $R = 0.058$ and $R_w = 0.052$. Crystallographic data for the structure of **3** have been deposited with the *CCDC* (No. 133400). Copies of the data can be obtained free of charge at the address given above under **2**.

Crystal Data for **4**: At $-115°$ with MoK_α radiation: $a = 1391.5(3)$, $b = 846.2(2)$, $c = 2198.4(5)$ pm, $\beta =$ 99.722(5)°, monoclinic, $P2_1/c$, $Z = 4$, $\mu(Mo) = 1.46$ cm^{-1}, 2011 unique reflections with $I > 3\sigma(I)$. The structure was solved by direct methods (MULTAN) and refined by full-matrix least-squares analysis on *F.* S, O, C, and N were refined with anisotropic thermal parameters. H-Atoms were modeled in fixed positions. The largest residual electron density in the final difference *Fourier* map was 0.33 e/Å^3 near O^2. The data/parameter ratio was 6.73. The final *R* factors were $R = 0.055$ and $R_w = 0.056$. Crystallographic data for the structure of **4** have been deposited with the *CCDC* (No. 133401). Copies of the data can be obtained free of charge at the address given above under **2**.

Crystal Data for **6 · MeCN**. At −70° with MoK_α radiation: $a = 1700.0(2)$, $b = 677.6(1)$, $c = 1794.9(1)$ pm, orthorhombic, *Pnma*, $Z = 4$, µ(Mo) = 0.67 cm^{-1}, 1164 unique reflections with $I > 3\sigma(I)$. The structure was solved by direct methods (MULTAN) and refined by full-matrix least-squares analysis on *F.* C and N were refined with anisotropic thermal parameters. H-Atoms were refined with isotropic thermal parameters. The largest residual electron density in the final difference *Fourier* map was 0.31 e/Å^3 near N(3). The data/parameter ratio was 5.06. The final *R* factors were $R = 0.053$ and $R_w = 0.050$. Crystallographic data for the structure of **6 · CH_3CN** have been deposited with the *CCDC* (No. 133402). Copies of the data can be obtained free of charge at the address given above under **2**.

Crystal Data for **10 · BPh_4**: At −70° with MoK_α radiation: $a = 2361.8(5)$, $b = 1068.8(2)$, $c = 1120.8(2)$ pm, orthorhombic, *Pnma*, $Z = 4$, µ(Mo) = 2.51 cm^{-1}, 1684 unique reflections with $I > 3\sigma(I)$. The structure was solved by direct methods (MULTAN) and refined by full-matrix least-squares analysis on *F.* C, Cl, B, and N were refined with anisotropic thermal parameters. H-Atoms were refined with isotropic thermal parameters. The largest residual electron density in the final difference *Fourier* map was 0.59 e/Å^3. The data/parameter ratio was 6.40. The final *R* factors were $R = 0.055$ and $R_w = 0.053$. Goodness of fit = 1.83. Crystallographic data for the structure of **10 · BPh_4** have been deposited with the *CCDC* (No. 133403). Copies of the data can be obtained free of charge at the address given above under **2**.

Crystal Data for **11 · Cl**: At −70° with MoK_α radiation: $a = 625.5(1)$, $b = 909.2(1)$, $c = 1003.3(2)$ pm, $\alpha = 105.11(1)°$, $\beta = 106.57(1)°$, $\gamma = 105.10(1)°$, triclinic, $P\bar{1}$, $Z = 2$, µ(Mo) = 3.72 cm^{-1}, 2370 unique reflections with $I > 3\sigma(I)$. The structure was solved by direct methods (MULTAN) and refined by full-matrix least-squares analysis on *F.* C, Cl, F, and N were refined with anisotropic thermal parameters. H-Atoms were refined with isotropic thermal parameters. The largest residual electron density in the final difference *Fourier* map was 0.31 e/Å^3 near C^2. The data/parameter ratio was 13.94. The final *R* factors were $R = 0.031$ and $R_w = 0.043$. Goodness of fit = 2.05. Crystallographic data for the structure of **11 · Cl** have been deposited with the *CCDC* (No. 133404). Copies of the data can be obtained free of charge at the address given above under **2**.

REFERENCES

[1] A.J. Arduengo, III, *Acc. Chem. Res.* **1999**, *32*, 913.
[2] A. J. Arduengo, III, R. Krafczyk, *Chemie in unserer Zeit* **1998**, *32*, 6.
[3] W. A. Herrmann, C. Köcher, *Angew. Chem., Int. Ed*. **1997**, *36*, 2162.
[4] X. M. Du, H. Fan, J. L. Goodman, M. A. Kesselmayer, K. Krogh-Jespersen, J. A. LaVilla, R. A. Moss, S. Shen, R. S. Sheridan, *J. Am. Chem. Soc*. **1990**, *112*, 1920.
[5] R. A. Moss, S. Shen, M. Wlostowski, *Tetrahedron Lett*. **1988**, *29*, 6417.
[6] R. A. Moss, *Chem. Eng. News* **1969**, *47*, 50.
[7] J. P. Pezacki, *Can. J. Chem*. **1999**, *77*, 1230.
[8] H.-W. Wanzlick, H. Ahrens, *Chem. Ber*. **1966**, *99*, 1580.
[9] H.-W. Wanzlick, H.-J. Kleiner, *Chem. Ber*. **1963**, *96*, 3024.
[10] H.-W. Wanzlick, E. Schikora, *Chem. Ber*. **1961**, *94*, 2389.
[11] D. Enders, K. Breuer, J. Runsink, J. H. Teles, *Liebigs Ann. Chem.* **1996**, 2019.
[12] H.-W. Wanzlick, H. Ahrens, *Chem. Ber*. **1964**, *97*, 2447.
[13] A. J. Arduengo, III, R. L. Harlow, M. Kline, *J. Am. Chem. Soc*. **1991**, *113*, 361.
[14] H.-W. Wanzlick, *Angew. Chem*. **1962**, *74*, 128.
[15] H.-W. Wanzlick, F. Esser, H.-J. Kleiner, *Chem. Ber*. **1963**, *96*, 1208.
[16] A. J. Arduengo, III, F. Davidson, H. V. R. Dias, J. R. Goerlich, D. Khasnis, W. J. Marshall, T. K. Prakasha, *J. Am. Chem. Soc*. **1997**, *119*, 12742.
[17] G. A. Landrum, N. Goldberg, R. Hoffmann, *J. Chem. Soc., Dalton Trans.* **1997**, 3605.
[18] A. J. Arduengo, III, M. Tamm, J. C. Calabrese, *J. Am. Chem. Soc*. **1994**, *116*, 3625.
[19] A. J. Arduengo, III, S. F. Gamper, M. Tamm, J. C. Calabrese, F. Davidson, H. A. Craig, *J. Am. Chem. Soc*. **1995**, *117*, 572.

[20] S. Scheiner, *Acc. Chem. Res.* **1994**, *27*, 402.
[21] C. Wakselman, A. Lantz, 'Perfluoroalkyl bromides and iodides' in 'Organofluorine Chemistry: Principles and Commercial Applications', R. E. Banks, B. E. Smart, J. C. Tatlow, Ed.; Plenum Press: New York, 1994, 180.
[22] A. A. Sivakov, V. N. Chistokletov, A. Y. Platonov, E. D. Maiorova, *Zh. Org. Khim*. **1994**, *30*, 947.
[23] S. V. Shelyazhenko, Y. A. Fialkov, L. M. Yagupol'skii, *Zh. Org. Khim.* **1992**, *28*, 1652.
[24] I. Rico, C. Wakselman, *Tetrahedron Lett*. **1981**, *22*, 323.
[25] A. J. Arduengo, III, J. R. Goerlich, D. Khasnis, M. Tamm, unpublished results.

Received September 2, 1999